Nov 11th, 12:00 AM

Web Crippling Strength of High Strength Steel Beams

Chiravut Santaputra

M. Brad Parks

Wei-wen Yu
Missouri University of Science and Technology, wwy4@mst.edu

Eighth International Specialty Conference on Cold-Formed Steel Structures
St. Louis, Missouri, U.S.A., November 11-12, 1986

WEB CRIPPLING STRENGTH OF HIGH STRENGTH STEEL BEAMS

by

C. Santaputra,[1] M. B. Parks,[2] and W. W. Yu[3]

INTRODUCTION

In recent years, high strength steels have been widely used in automotive structural components to achieve weight reduction while complying with federal safety standards. The current American Iron and Steel Institute (AISI) design recommendation, "Guide for Preliminary Design of Sheet Steel Automotive Structural Components" (1) is based primarily on the 1968 Edition of the AISI Specification (2) which was written for the design of buildings. The AISI 1981 Guide is applicable to materials with yield strengths up to 80 ksi (552 MPa).

Because some of the design criteria for web crippling were revised in the 1980 and 1986 Editions of the AISI Specification (3,4), and because high strength steels with yield strengths from 80 to 190 ksi (552 to 1310 MPa) are now used for automotive structural components (5-10), a comprehensive design guide is highly desirable.

Recently, a research project entitled "Design of Automotive Structural Components Using High Strength Sheet Steels" has been conducted at the University of Missouri-Rolla under the sponsorship of AISI. The main purpose of the project has been to develop additional design criteria for the use of a broader range of high strength steels. Web crippling and a combination of web crippling and bending moment is one area that has been studied as a part of the research project.

This paper presents the results of tests carried out to determine the web crippling strength of webs of cold-formed steel beams fabricated from high strength sheet steels commonly used in the automobile industry.

---

[1]Research Assistant, Department of Civil Engineering, University of Missouri-Rolla, Rolla, Missouri.

[2]Research Assistant, Department of Civil Engineering, University of Missouri-Rolla, Rolla, Missouri.

[3]Curators' Professor of Civil Engineering, University of Missouri-Rolla, Rolla, Missouri.

Various loading arrangements were performed in the experimental study. New design criteria to prevent web crippling and a combination of web crippling and bending moment are proposed.

EXPERIMENTAL INVESTIGATION

The theoretical analysis concerning web crippling of cold-formed steel beams is extremely complicated. There exists no exact or closed form solution to the problem. Because of mathematical difficulties encountered, the present AISI design provisions for web crippling are based on extensive experimental investigations conducted at Cornell University, University of Missouri-Rolla (UMR), other institutions and individual steel companies (11). However, all of the mentioned web crippling research work has been for materials with relatively low strengths. In this paper, web crippling tests of materials with yield strengths of 60 to 165 ksi (414 to 1138 MPa) are discussed.

In the present study, web crippling tests were carried out for the following four basic loading conditions:

1. Interior one-flange loading (IOF)
2. End one-flange loading (EOF)
3. Interior two-flange loading (ITF)
4. End two-flange loading (ETF)

In order to avoid the problem of discontinuity between the web crippling equations for the above basic loading conditions, additional tests were performed for the transition ranges.

Two types of sections were tested. Hat sections, as shown in Fig. (1a), were tested in order to study single unreinforced webs. For sections that provide a high degree of restraint against rotation of the webs, I-beams (Fig. 1b) were tested. The experimental investigations are summarized as follows:

A. TEST SPECIMENS

Hat sections and I-beams were fabricated from five different types of high strength sheet steels. Table 1 shows three different profiles for each type of cross sections that were used in this study. The materials used to form these specimens included hot-rolled and cold-rolled sheet steels having yield strengths ranging from 58.2 to 165.1 ksi

(401 to 1138 MPa). Table 2 gives the mechanical properties and thicknesses of these sheet steels. Because all specimens were formed by a press-braked operation, there was little or no cold working effect except in the corners.

All I-beam specimens were fabricated from two identical channels connected back to back by self-tapping screws (14 x 3/4 Tek screws) located at a distance of 1/2 in. (12.7 mm) from top and bottom flanges. The self-tapping screws were spaced along the beam length at a constant distance of 2 in. (50.8 mm) from center to center. In order to minimize the initial deformations, the screws were driven from alternate sides of the webs.

The pilot tests of I-beam specimens indicated that there was premature failure caused by rotation of the flanges about the screw lines. The premature failure was caused by the large bend radii, which is required for the high strength and low ductility sheet steels. This type of failure is also a function of the distance between the flanges and screw lines. Figure 2 shows the sketch of this type of failure. In order to prevent this premature failure before web crippling could be developed, bearing plates were attached to flanges of I-beams.

For hat sections, the lower unstiffened flanges were connected by 1/8 x 3/4 in. (3.175 x 19.05 mm) rectangular bars at appropriate locations to maintain the shape of the cross sections during the test.

B. TEST PROCEDURE

All tests were performed in a 120,000 pound (533,770 N) Tinius Olsen universal testing machine. All specimens were loaded to failure. During the test, loads were applied slowly at an increment of approximately 15% of the predicted ultimate loads and maintained constant at each load level for 5 minutes.

Vertical movement of the bearing plate by which the load was applied was recorded at each step to detect the load and time at which the bearing plate started to penetrate into the web.

Lateral deformation of the webs of hat sections at the location of expected failure was measured. The lateral movement was measured at 1/2 in. (12.7 mm) spacing along the center line of the bearing plate by an LVDT. Readings were taken at each load interval. For the I-beam specimens, there was no lateral movement of the webs until the ultimate loads were reached.

Vertical strain distribution in the web at the bearing plate was also investigated by attaching strain gages to some of the hat sections. For each of the specimens studied, three pairs of strain gages were attached back to back vertically along a horizontal line at a distance of 1/4 in. (6.35 mm) from the center of the gages to the web-flange junction.

Details of the test arrangement for each loading condition are as follows:

1. Interior One-Flange Loading (IOF)

All specimens were tested as simply supported flexural members subjected to a concentrated load as shown in Fig. 3a. A total of 36 hat sections and 24 I-beams were loaded at mid-span with the clear distance between opposite bearing plates (e_1 and e_2) of 1.5h, where h is the clear distance between flanges measured along the plane of the web. An additional 36 hat sections were tested under unsymmetric loading, in which e_1 varied from 0.75h to 1.25h and e_2 varied accordingly from 2.25h to 1.75h.

A 2-in. (50.8-mm) bearing plate was under the applied concentrated load while 4-in. (101.6-mm) bearing plates were used at both ends. In order to prevent end failure from occuring before the expected interior failure developed, wood blocks were inserted at both ends of the specimens.

2. End One-Flange Loading (EOF)

For this loading condition, 30 hat sections and 24 I-beams were tested as simply supported flexural members subjected to a concentrated load at mid-span (Fig. 3b). A 4-in. (101.6-mm) bearing plate was under the concentrated load while 2-in. (50.8-mm) bearing plates were used at both ends. The clear distance between the opposite bearing plates was set at 1.5h.

3. Interior Two-Flange Loading (ITF)

A total of 24 specimens for both hat sections and I-beams were tested as shown in Fig. 3c. Two 2-in. (50.8-mm) bearing plates were used in the middle of the specimens for both top and bottom flanges. The designed clear distance between the edge of bearing plates to the end of the specimens was 1.5h.

4. End Two-Flange Loading (ETF)

The numbers of specimens are the same as the ITF case. It can be seen from Fig. 3d that two 2-in. (50.8-mm) bearing plates were used at one end of the specimens. At the unloaded end of the specimens, an elastic support was used to keep the specimens in a horizontal position throughout the test.

5. Transition between Interior One-Flange Loading and Interior Two-Flange Loading

For the transition ranges, six hat sections were tested for each case. Figure 3e shows the test arrangement which was the same as that of the IOF case except that one end bearing plate was moved in order to vary the clear distance between the opposite bearing plates from 0.1h to 0.75h. The expected failure was under the applied concentrated load.

6. Transition between Interior One-Flange Loading and End One-Flange Loading

Test setup was the same as that of the EOF case except that the end bearing plates were moved closer to the bearing plate under the applied concentrated load (Fig. 3f). Failure was expected at the reaction.

7. Transition between End One-Flange Loading and End Two-Flange Loading

As in the previous case, the test arrangement was the same as that of the EOF case but the bearing plate under the applied concentrated load was moved closer to one end of the specimen (Fig. 3g). The expected failure was at the end bearing plate closer to the applied load.

C. TEST RESULTS

The ultimate web crippling loads were recorded for all tests. Lateral deformations of the webs and vertical deflections of the beams were recorded as discussed earlier. Because the specimens were unstable at the ultimate loads, all deflection and deformation measurements could not be obtained at this load level.

The nature of failure was carefully inspected throughout the tests. The following two types of web crippling failure were observed.

1. Overstressing (Bearing) Failure

Failure of this type occurred just under the bearing plates with relatively small lateral deformations of the webs of the hat sections. For I-beam specimens, no lateral movement of the webs was observed before

the ultimate loads were reached. The applied load increased steadily up to the ultimate load and remained at that level for a long period of time while the bearing plate gradually penetrated into the web. It was believed that overstressing of the web underneath the bearing plate caused this type of failure.

2. Buckling Failure

For this type of failure, the load increased steadily up to the ultimate load. At the ultimate load, the web became unstable and the load dropped suddenly. There were relatively large lateral deformations of the webs of the hat sections even before failure. Paired strain gages which were attached to the webs of some of hat sections indicated that the strains caused by bending of the web was much more pronounced than the strain caused by vertical compressive stress. However, little, if any, lateral deformations occurred in the webs of the I-beams prior to buckling.

Figures 4 and 5 show the typical failure for each case of the four basic loading conditions for hat sections and I-beams, respectively.

D. EVALUATION OF EXPERIMENTAL DATA

The results of tests obtained from this phase of investigation were evaluated by comparing the tested failure loads to the predicted ultimate web crippling loads based on the AISI 1981 Guide (1) and the 1980 Specification (3). These comparisons are discussed below for each type of sections. It should be noted that the empirical expressions for these predictions were derived from test data with yield strengths ranging from 30 to 57 ksi (207 to 393 MPa) which are applicable to building products.

1. Hat Sections

For hat sections formed from very high strength sheet steels, the web crippling loads are underestimated. This underestimation is caused by the yield strength functions used in the equations to predict the ultimate web crippling loads. The effect of yield strength on the ultimate web crippling load is the same in both Refs. 1 and 3. The functions of yield strength for interior and end loading conditions can be expressed as Eqs. (1) and (2), respectively.

$$f_1(F_y) = \{1.22-.22(F_y/33)\}(F_y/33) \quad (1)$$

$$f_2(F_y) = \{1.33-.33(F_y/33)\}(F_y/33) \quad (2)$$

According to these two equations, the ultimate web crippling load for a given section increases as the yield strength, F_y, increases up to a certain value, beyond which the ultimate web crippling load decreases as the yield strength increases. The functions $f_1(F_y)$ and $f_2(F_y)$ reach their maximum values when F_y is 91.5 and 66.5 ksi (630.8 and 458.5 MPa), respectively. In this evaluation, when the actual yield strength is greater than this limit the value of 91.5 or 66.5 ksi (630.8 or 458.5 MPa) was used in lieu of the actual value of F_y.

Even though the above modifications of the yield strength functions were used, the inaccuracy of the predicted web crippling loads still persisted. This may be due to the fact that some specimens have a buckling type failure.

2. I-Beams

The predicted ultimate web crippling loads based on the 1981 Guide overestimate the failure loads with the degree of accuracy decreasing as the yield strength increases for all four loading cases. Also, the predicted web crippling loads based on the 1980 Specification have the same trend of inaccuracy. This overestimation resulted mainly from using the yield strength, F_y, as a parameter in the prediction equations even though most of the specimens have a buckling type failure.

For the cases of ITF and ETF, the equations based on the 1980 Specification are independent of F_y which is consistent with the observations made in this phase of study. The inaccuracy in predictions for these cases may result from using inappropriate parameters for the buckling type failure.

DEVELOPMENT OF NEW EQUATIONS

As discussed earlier, even though the present AISI design criteria for web crippling can be used for the design of buildings, they are not suitable for application with sections fabricated from very high strength materials. In order to cover a wider range of material

strengths, new prediction equations were developed. The new equations distinguish between overstressing (bearing) and buckling failure. These equations were developed on the basis of the available data obtained from the following sources:

1. previous Cornell and UMR tests reported in Ref. 12,
2. recent UMR tests conducted by Lin and reported in Ref. 13, and
3. tests of high strength sections conducted in this study.

The parameters used in the derivation of the new equations are nondimensional terms. A nonlinear least squares iteration technique was used to determine the empirical constants. The form for each type of equation is discussed as follows:

1. Overstressing (Bearing) Failure

The basic nondimensional parameters used in this paper are $P/(t^2F_y)$, N/t, and R/t. For this type of failure the ratio h/t has little or no effect on the ultimate web crippling load. All data used for the interior one-flange loading case were selected in such a way that the ratio M/M_u was less than 0.3. Previous research work indicated that when the moment ratio is less than this limit there is little or no interaction between web crippling and bending moment. Equation (3) deals with this type of failure.

$$\{P_{cy}/(t^2F_y)\} = f(N/t, R/t) \tag{3}$$

2. Buckling Failure

The design equation for buckling failure was developed by using the same form of equation as that used for buckling of a rectangular flat plate subjected to partial edge loading (14,15) except that the length-to-depth ratio (L/h) was replaced by the clear distance between the opposite bearing plates-to-depth ratio (e/h). By using this parameter, the equations can be applied to either symmetric or unsymmetric loading. This type of equation can be written as

$$\{P_{cb}/(Et^2)\} = f(N/h, h/t, e/h). \tag{4}$$

3. Combined Bending and Web Crippling

To be consistent with the current AISI Specification, the interaction equations were determined in terms of the moment ratio (M/M_u) and the load ratio (P_{mc}/P_{cy}) as given below:

$$(M/M_u) + A(P_{mc}/P_{cy}) \leq C. \quad (5)$$

In the above equation, A and C are constants to be determined by regression analysis. The predicted combined bending and web crippling load, P_{mc}, determined from Eq. (5) must be checked against P_{cb} of the interior one-flange loading case. The smaller value between these predicted loads governs the design.

All of the newly developed equations are included in the design recommendations which are proposed in this paper. The predicted ultimate web crippling loads based on these newly developed equations give good agreements with the tested failure loads for all cases with yield strengths from 30 to 165 ksi (207 to 1138 MPa). Figures 6a to 6h show the effect of the material yield strength, F_y, on the ratio of the tested failure loads to the predicted ultimate web crippling loads, P_t/P_c, for the test data used in the development of the prediction equations. These equations were also verified by tests using high and ultra high strength materials which were conducted at Inland Steel Company (6) and Ford Motor Company(7). Complete details of the test data and further comparisons of the tested and predicted failure loads are documented in Ref. 16.

PROPOSED DESIGN RECOMMENDATIONS

Based on the research findings, design methods intended to cover all possibile failure modes of web crippling and a combination of web crippling and bending moment were developed. It should be noted that the following design equations predict the ultimate strength without any factor of safety:

A. CONCENTRATED LOADS AND REACTIONS

The ultimate strengths of unreinforced beam webs subjected to concentrated loads or reactions can be estimated by the equations given in Design Recommendation A for beams having single webs and in Design Recommendation B for I-beams with flanges connected to bearing plates. The equations apply to beams when $F_y \leq 190$ ksi (1310 MPa), $h/t \leq 200$, $N/t \leq 100$, $N/h \leq 2.5$, and $R/t \leq 10$.

The design methods for web crippling were categorized into nine cases depending on the values of e and Z (Figs. 7-10). The equations used for Cases 1, 2, 4, and 5 were derived from the test data obtained from four basic loading conditions classified as end one-flange loading, interior one-flange loading, end two-flange loading, and interior two-flange loading, respectively. Cases 3, 6, 7, 8, and 9 represent the transitions of four basic loading conditions and can be determined by using simple interpolation.

Design Recommendation A

Ultimate Concentrated Loads and Reactions for
Shapes Having Single Unreinforced Webs

$e \geq .5h$	1) $Z = 0$: $(P_c)_1$ is the smaller of P_{cy} or P_{cb} where $P_{cy} = 9.9t^2F_yc_{11}c_{21}(\sin\theta)$ (6) $P_{cb} = 0.047Et^2c_{41}c_{51}(\sin\theta)$ (7)
	2) $Z \geq 0.5h$: $(P_c)_2$ is the smaller of P_{cy} or P_{cb} where $P_{cy} = 7.80t^2F_yc_{12}c_{22}(\sin\theta)$ (8) $P_{cb} = 0.028Et^2c_{32}c_{42}c_{52}(\sin\theta)$ (9)
	3) $0 < Z < .5h$: $(P_c)_3 = (P_c)_1 + ((P_c)_2-(P_c)_1)(Z/.5h)$
$e = 0$	4) $Z = 0$: $(P_c)_4 = P_{cb}$ where $P_{cb} = 0.011Et^2c_{33}c_{43}c_{73}(\sin\theta)$ (10)
	5) $Z \geq .5h$: $(P_c)_5$ is the smaller of P_{cy} or P_{cb} where $P_{cy} = 7.8t^2F_yc_{12}c_{22}(\sin\theta)$ (11) $P_{cb} = 0.0041Et^2c_{34}c_{44}c_{64}(\sin\theta)$ (12)
	6) $0 < Z < .5h$: $(P_c)_6 = (P_c)_4 + ((P_c)_5-(P_c)_4)(Z/.5h)$
$0 < e < .5h$	7) $Z = 0$: $(P_c)_7 = (P_c)_4 + ((P_c)_1-(P_c)_4)(e/.5h)$
	8) $Z \geq .5h$: $(P_c)_8 = (P_c)_5 + ((P_c)_2-(P_c)_5)(e/.5h)$
	9) $0 < Z < .5h$: $(P_c)_9 = (P_c)_6 + ((P_c)_3-(P_c)_6)(e/.5h)$

Design Recommendation B

Ultimate Concentrated Loads and Reactions for
I-Beams with Unreinforced Webs

$e \geq .5h$	1) $Z = 0$: $(P_c)_1 = P_{cb}$ where $P_{cb} = 0.063Et^2c_{45}c_{55}$ (13)
	2) $Z \geq 0.5h$: $(P_c)_2$ is the smaller of P_{cy} or P_{cb} where $P_{cy} = 15t^2F_yc_{12}$ (14) $P_{cb} = 0.032Et^2c_{36}c_{46}$ (15)
	3) $0 < Z < .5h$: $(P_c)_3 = (P_c)_1 + ((P_c)_2-(P_c)_1)(Z/.5h)$
$e = 0$	4) $Z = 0$: $(P_c)_4 = P_{cb}$ where $P_{cb} = 0.015Et^2c_{37}c_{47}$ (16)
	5) $Z \geq .5h$: $(P_c)_5$ is the smaller of P_{cy} or P_{cb} where $P_{cy} = 15t^2F_yc_{12}$ (17) $P_{cb} = 0.051Et^2c_{38}c_{48}c_{68}$ (18)
	6) $0 < Z < .5h$: $(P_c)_6 = (P_c)_4 + ((P_c)_5-(P_c)_4)(Z/.5h)$
$0 < e < .5h$	7) $Z = 0$: $(P_c)_7 = (P_c)_4 + ((P_c)_1-(P_c)_4)(e/.5h)$
	8) $Z \geq .5h$: $(P_c)_8 = (P_c)_5 + ((P_c)_2-(P_c)_5)(e/.5h)$
	9) $0 < Z < .5h$: $(P_c)_9 = (P_c)_6 + ((P_c)_3-(P_c)_6)(e/.5h)$

In Design Recommendations A and B,

E = modulus of elasticity of steel = 29,500 ksi (203,373 MPa)

e = clear distance between edges of the adjacent opposite bearing plates, in.. For reactions or concentrated loads on cantilevers, see Fig. 7. For interior concentrated load shown in Fig. 8, e is taken as the smaller value of e_1 and e_2.

F_y = yield strength of the web, ksi

h = clear distance between flanges measured along the plane of web, in.

N = actual length of bearing, in.

P_c = governing ultimate web crippling load, per web, kips

P_{cb} = web crippling load caused by buckling, per web, kips

P_{cy} = web crippling load caused by bearing, per web, kips

R = inside bend radius, in.

t = web thickness, in.

Z = distance between the edge of the bearing plate to the near end of the beam, in.. See Figs. 7 and 8.

Z_1 = distance between the edge of the bearing plate to the far end of the beam, in.. See Fig. 7.

θ = angle between plane of web and plane of bearing surface > 45 but no more than 90, degrees

$c_{11} = 1+.0122(N/t) \leq 2.22$

$c_{12} = 1+.217(N/t)^{.5} \leq 3.17$

$c_{21} = 1-.247(R/t) \geq 0.32$

$c_{22} = 1-.0814(R/t) \geq 0.43$

$c_{32} = 1+2.4(N/h) \leq 1.96$

$c_{33} = 1+.54(N/h) \leq 1.41$

$c_{34} = 1+.729(N/h) \leq 1.30$

$c_{36} = 1+1.318(N/h) \leq 1.53$

$c_{37} = 1+1.262(N/h)^{1.5} \leq 1.82$

$c_{38} = 1+.109(N/h)^{3} \leq 2.69$

$c_{41} = 1-.00348(h/t) \geq 0.32$

$c_{42} = 1-.00170(h/t) < 0.81$

$c_{43} = 1-.00245(h/t) \geq 0.51$

$c_{44} = 1-.0000141(h/t)^2 \geq 0.44$

$c_{45} = 1-.00118(h/t) \leq 0.82$

$c_{46} = 1-.000471(h/t) \leq 0.95$

$c_{47} = 1-.0017(h/t) \geq 0.66$

$c_{48} = 1-.0060(h/t) \geq 0.46$

$c_{51} = 1-.298(e/h) \geq 0.52$

$c_{52} = 1-.120(e/h) \geq 0.40$

$c_{55} = 1-.233(e/h) \geq 0.58$

$c_{64} = 1+4.547(Z/h) \leq 7.82$

$c_{68} = 1+0.109(Z/h) \leq 1.22$

$c_{73} = 1+.56(Z_1/h) \leq 1.98$

For uniform loading, the distance "e" should be considered as follows:

a. For end reactions, e is taken as half of the clear distance between the adjacent bearing plates, see Fig. 9, i. e., $e = L_n/2$.

b. For interior reactions (Fig. 10), e is taken as the larger value of $L_{n1}/2$ and $L_{n2}/2$.

B. COMBINED BENDING AND WEB CRIPPLING

Unreinforced flat webs of shapes subjected to a combination of bending and reaction or concentrated load shall be designed to meet the following requirements:

1. Shapes Having Single Webs

$$(M/M_u) + 1.10(P_{mc}/P_{cy}) \leq 1.42 \qquad (19)$$

where M = applied bending moment, at or immediately adjacent to the point of application of the concentrated load or reaction, P_{mc}, kip-in.

M_u = ultimate bending moment permitted if bending stress only exists, kip-in.

P_{mc} = concentrated load or reaction in the presence of bending

moment, kips

P_{cy} = concentrated load or reaction in the absence of bending moment determined from Eq. (8), kips

The value of P_{mc} determined from Eq. (19) shall not be larger than P_{cb} calculated from Eq. (9).

2. I-BEAMS

$$(M/M_u) + 1.07(P_{mc}/P_{cy}) \leq 1.28 \qquad (20)$$

where P_{cy} shall be determined from Eq. (14). The value of P_{mc} determined from Eq. (20) shall not be larger than P_{cb} calculated from Eq. (15). M and M_u are defined in Item 1 above.

CONCLUSIONS

The structural behavior of thin-walled, cold-formed steel beam webs subjected to concentrated loads or reactions was discussed. Web crippling tests of hat sections and I-beams fabricated from very high strength sheet steels under various loading conditions were performed. Test results indicated that the present AISI design criteria for web crippling are not suitable for application with sections cold-formed from very high strength sheet steels.

Empirical equations were derived to predict the ultimate web crippling loads based on the test data with a large range of yield strengths of materials. The new equations distinguish between overstressing (bearing) failure and buckling failure. Interaction equations for combined bending and web crippling were also derived for both hat sections and I-beams.

Tests for the transition ranges between the four basic loading conditions were also performed. It was found that by using a simple interpolation between the four basic loading conditions, reasonable accuracy of prediction can be achieved.

A new concept of design method was introduced. This method covers all possible web crippling design and can be applied to a wider range of material strengths than the present available design criteria.

ACKNOWLEDGMENTS

This investigation was sponsored by the American Iron and Steel Institute. The technical guidance provided by the AISI Task Force on Structural Design and Research of the Transportation Department, under the chairmanship of Dr. S. J. Errera, and the AISI staff, Dr. A. L. Johnson, is gratefully acknowledged.

Materials used in the experimental study were donated by Bethlehem Steel Corporation, Inland Steel Company and National Steel Corporation.

REFERENCES

1. American Iron and Steel Institute, "Guide for Preliminary Design of Sheet Steel Automotive Structural Components," 1981 Edition.
2. American Iron and Steel Institute, "Specification for the Design of Cold-Formed Steel Structural Members," 1968 Edition.
3. American Iron and Steel Institute, "Specification for the Design of Cold-Formed Steel Structural Members," 1980 Edition.
4. American Iron and Steel Institute, "Specification for the Design of Cold-Formed Steel Structural Members," 1986 Edition.
5. Errera, S. J., "Automotive Structural Design Using the AISI Guide," SAE Techanical Paper Series 820021.
6. Levy, B. S., "Advances in Designing Ultra High Strength Steel Bumper Reinforcement Beams," SAE Techanical Paper Series 830399.
7. Vecchio, M. T., "Design Analysis and Behavior of a Variety of As-Formed Mild and High Strength Sheet Materials in Large Deflection Bending," SAE Techanical Paper Series 830398.
8. American Iron and Steel Institute, "Steel Meets the Automotive Engineering Challenges" Supplemental Booklet Presented at the 1983 SAE Exposition.
9. Yu, W. W., Santaputra, C., and Parks, M. B., "Design of Automotive Structural Components Using High Strength Sheet Steels," First Progress Report, Civil Engineering Study 83-1, University of Missouri-Rolla, January 1983.

10. Santaputra, C., Parks, M. B., and Yu, W. W., "Web Crippling of Cold-Formed Steel Beams Using High Strength Sheet Steels," SAE Techanical Paper Series 860823.

11. Yu, W. W., Cold-Formed Steel Design, John Wiley & Sons, New York, 1985.

12. Hetrakul, N., and Yu, W. W., "Strucural Behavior of Beam Webs Subjected to Web Crippling and a Combination of Web Crippling and Bending," Final Report, Civil Engineering Study 78-4, University of Missouri-Rolla, June 1978.

13. Lin, S. H., "Structural Behavior of Cold-Formed Steel Beam Webs Subjected to Partial Edge Loading," Master Thesis, Civil Engineering Department, University of Missouri-Rolla, December 1984.

14. Khan, M. Z., and Walker, A. C., "Buckling of Plates Subjected to Localised Edge Loading," The Structural Engineer, vol. 50, June 1972.

15. Khan, M. Z., Johns, K. C., and Hayman, B., "Buckling of Plates with Partially Loaded Edges," Journal of the Structural Division, ASCE Proceedings, vol. 103, March 1977.

16. Santaputra, C., and Yu, W. W., "Design of Automotive Structural Components Using High Strength Sheet Steels: Web Crippling of High Strength Cold-Formed Steel Beams," Eighth Progress Report, Civil Engineering Study 86-1, University of Missouri-Rolla, to be published.

NOTATION

The following Symbols are used in this paper:

e Clear distance between edges of the adjacent opposite bearing plates, in.

E Modulus of elasticity of steel = 29,500 ksi (203,373 MPa)

F_y Yield strength, ksi

h Clear distance between flanges measured along the plane of the web, in.

L Total length of specimen, in.

M Applied bending moment, at or immediately adjacent to the point of

application of the concentrated load or reaction, kip-in.

M_u Ultimate bending moment if bending stress only exists, kip-in.

N Actual length of bearing, in.

P_c Governing ultimate web crippling load, kips

P_{cb} Ultimate web crippling load due to web buckling, kips

P_{cy} Ultimate web crippling load due to overstressing under the bearing plate, kips

P_{mc} Computed load for combined bending moment and web crippling, kips

R Inside bend radius, in.

t Base steel thickness, in.

Z Distance between the edge of the bearing plate to the near end of the beam, in.

Z_1 Distance between the edge of the bearing plate to the far end of the beam, in.

θ Angle between plane of web and plane of bearing surface, degrees.

TABLE 1a

Nominal Dimensions of Hat Sections Designed for Experimental Study

Profile No.	B1 (in.)	B2 (in.)	D1 (in.)	R (in.)
1	3.0	6.0	3.0	0.25
2	4.0	8.0	4.0	0.25
3	5.0	10.0	5.0	0.25

Notes: See Fig. 1a for definitions of symbols.
1 in. = 25.4 mm

TABLE 1b

Nominal Dimensions of I-Beams Designed for Experimental Study

Profile No.	B1 (in.)	D1 (in.)	R (in.)
1	3.0	3.0	0.25
2	4.0	4.0	0.25
3	5.0	5.0	0.25

Notes: See Fig. 1b for definitions of symbols.
1 in. = 25.4 mm

TABLE 2

Material Properties* and Thicknesses of Sheet Steels

Material	F_y (ksi)	F_u (ksi)	Elongation** (%)	t (in.)
80DK	58.2	87.6	25.7	0.048
80XF	77.1	89.1	20.4	0.088
100XF	113.1	113.1	8.1	0.062
140XF	141.2	141.2	4.4	0.047
140SK	165.1	176.2	4.3	0.046

* Material properties are based on the average longitudinal tension tests.
** Elongation in 2-in. gage length.
1 in. = 25.4 mm
1 ksi = 6.894 MPa

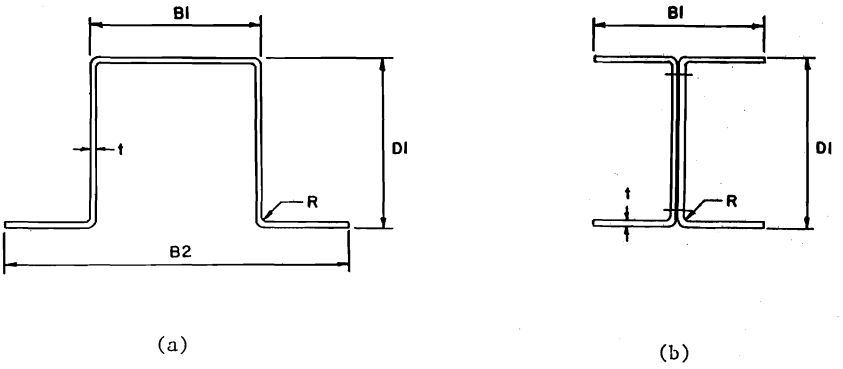

Fig. 1 Hat Sections and I-Beams Used in This Study

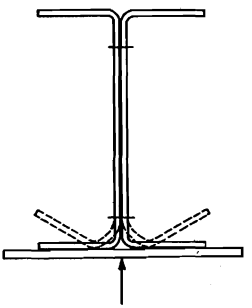

Fig. 2 Sketch Showing Bending Failure about Connection Line

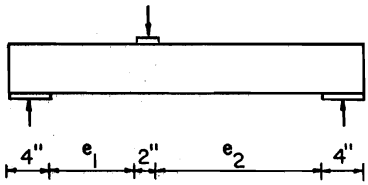

a) Interior One-Flange Loading (IOF)

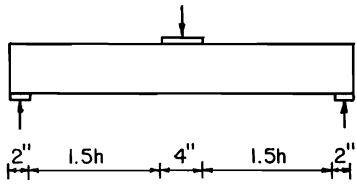

b) End One-Flange Loading (EOF)

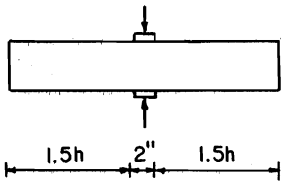

c) Interior Two-Flange Loading (ITF)

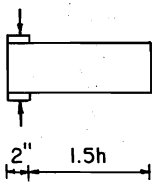

d) End Two-Flange Loading (ETF)

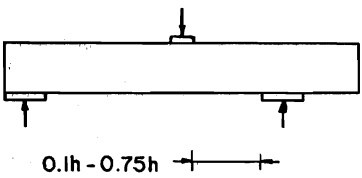

e) Transition between IOF and ITF

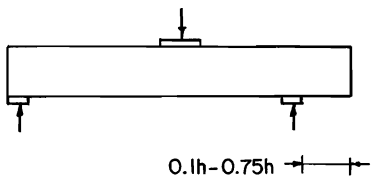

f) Transition between IOF and EOF

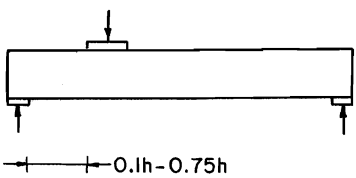

g) Transition between EOF and ETF

Fig. 3 Test Arrangements

a) Interior One-Flange Loading

b) End One-Flange Loading

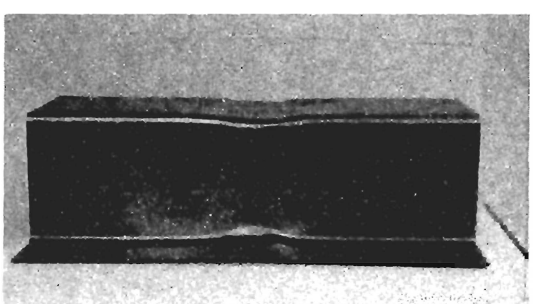

c) Interior Two-Flange Loading

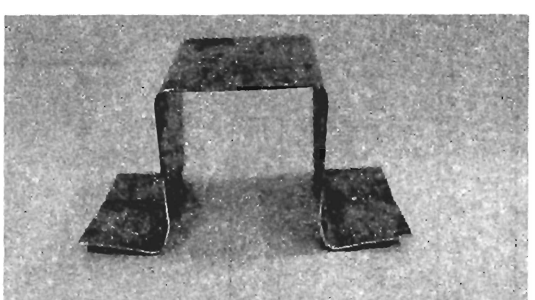

d) End Two-Flange Loading

Fig. 4 Typical Failure Modes of Hat Sections

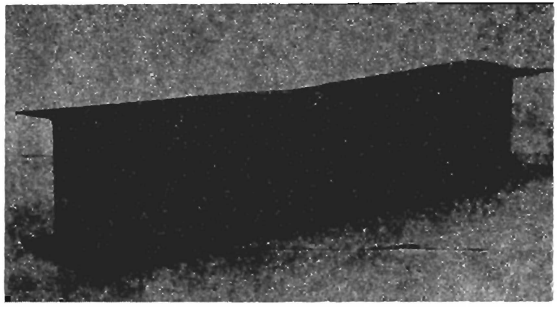

a) Interior One-Flange Loading

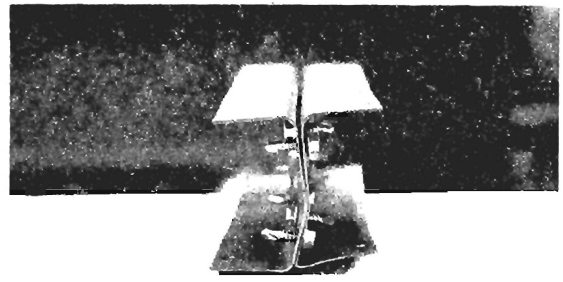

b) End One-Flange Loading

c) Interior Two-Flange Loading

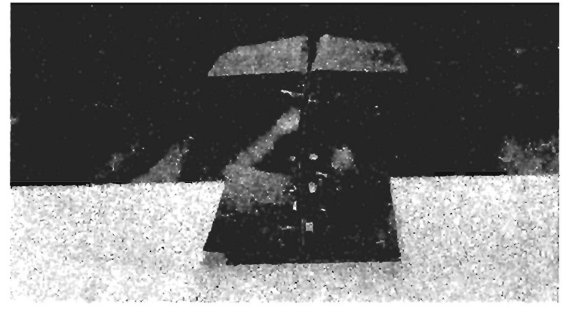

d) End Two-Flange Loading

Fig. 5 Typical Failure Modes of I-Beams

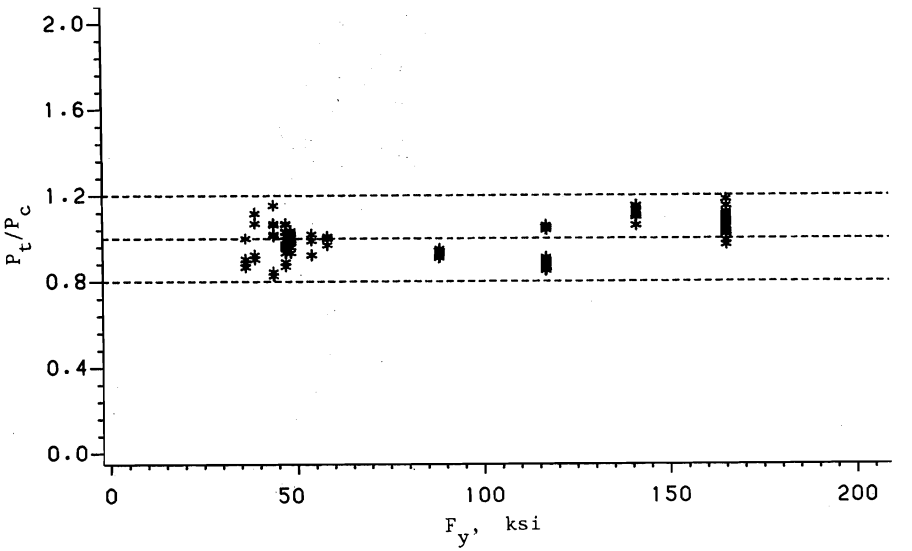

Fig. 6a Load Ratio, P_t/P_c, vs. Yield Strength, F_y, for Hat Sections Subjected to Interior One-Flange Loading

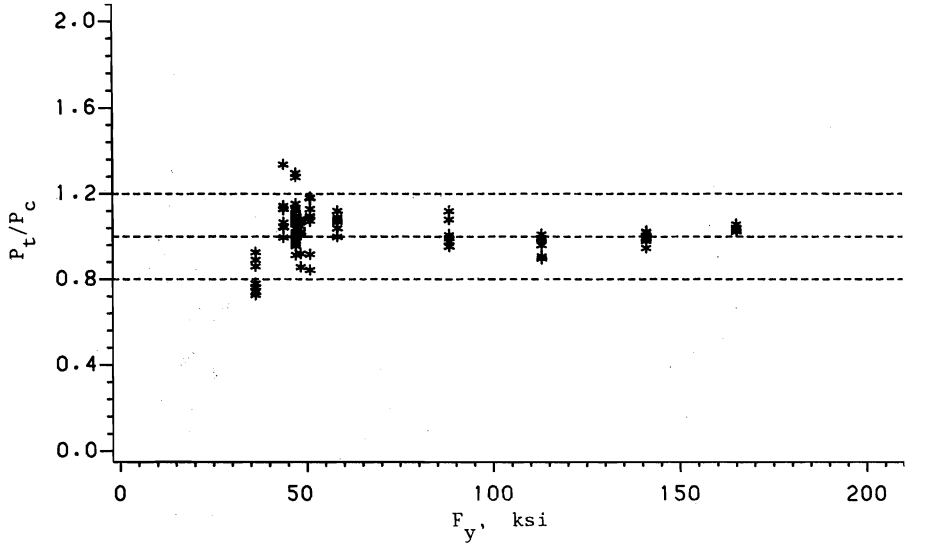

Fig. 6b Load Ratio, P_t/P_c, vs. Yield Strength, F_y, for Hat Sections Subjected to End One-Flange Loading

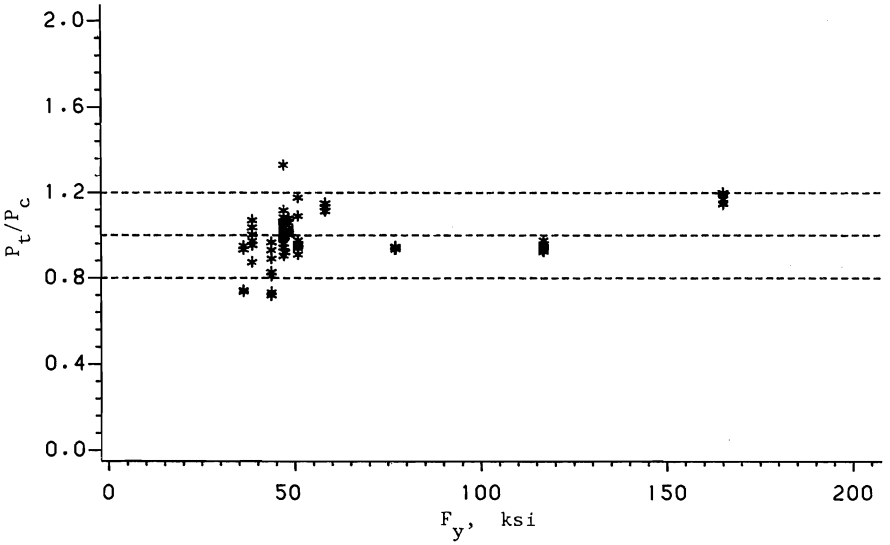

Fig. 6c Load Ratio, P_t/P_c, vs. Yield Strength, F_y, for Hat Sections Subjected to Interior Two-Flange Loading

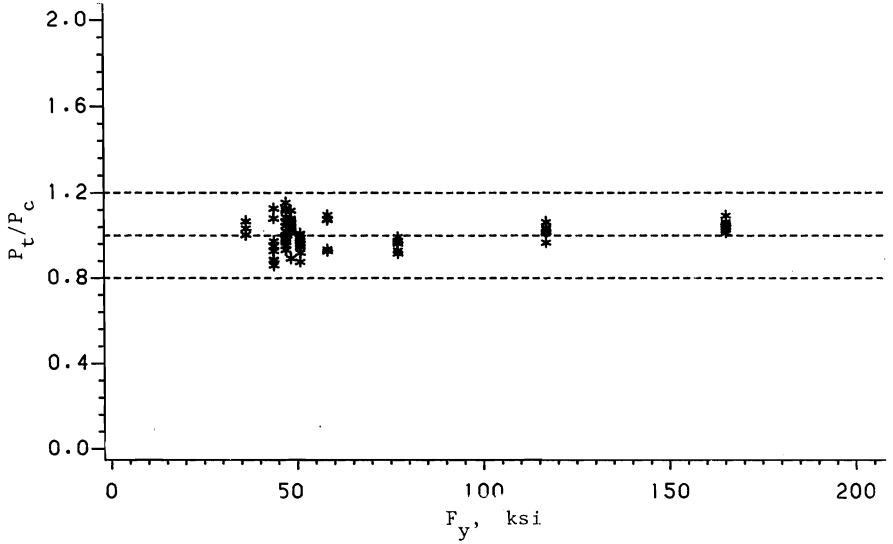

Fig. 6d Load Ratio, P_t/P_c, vs. Yield Strength, F_y, for Hat Sections Subjected to End Two-Flange Loading

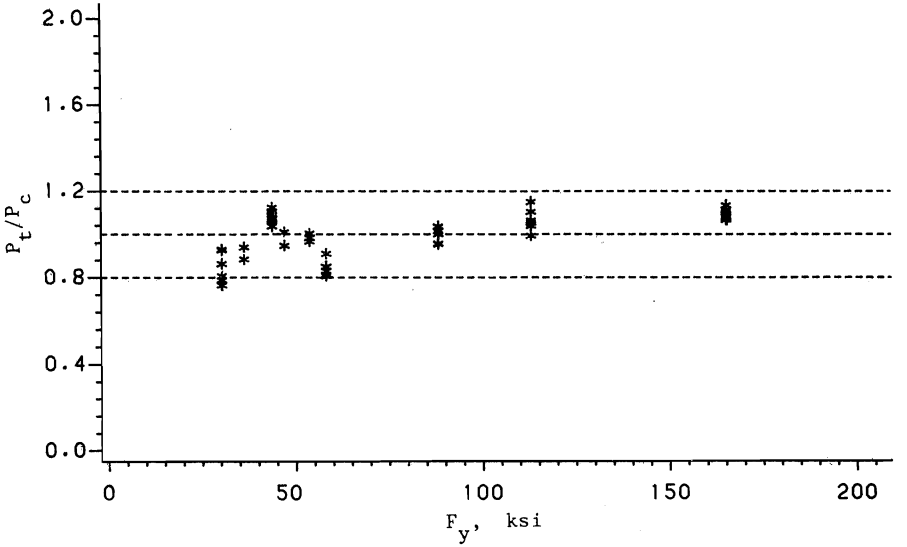

Fig. 6e Load Ratio, P_t/P_c, vs. Yield Strength, F_y, for I-Beams Subjected to Interior One-Flange Loading

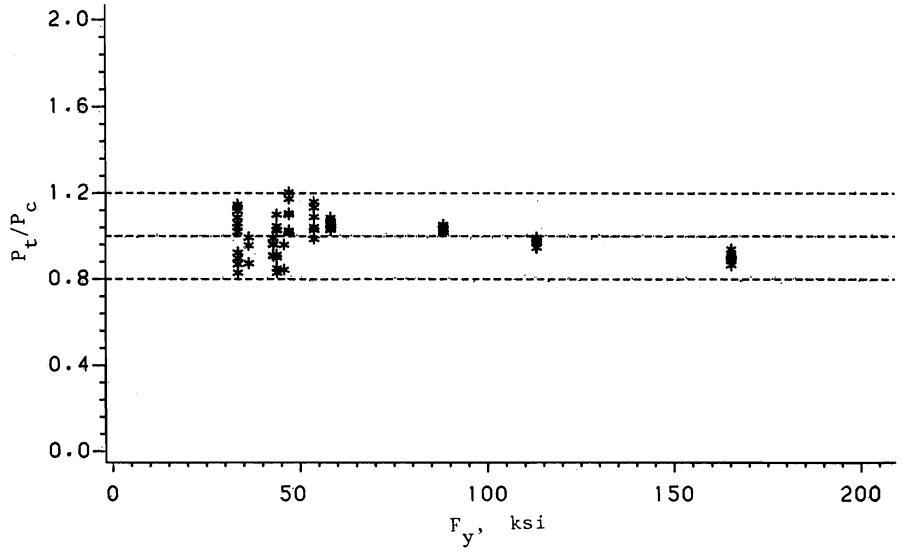

Fig. 6f Load Ratio, P_t/P_c, vs. Yield Strength, F_y, for I-Beams Subjected to End One-Flange Loading

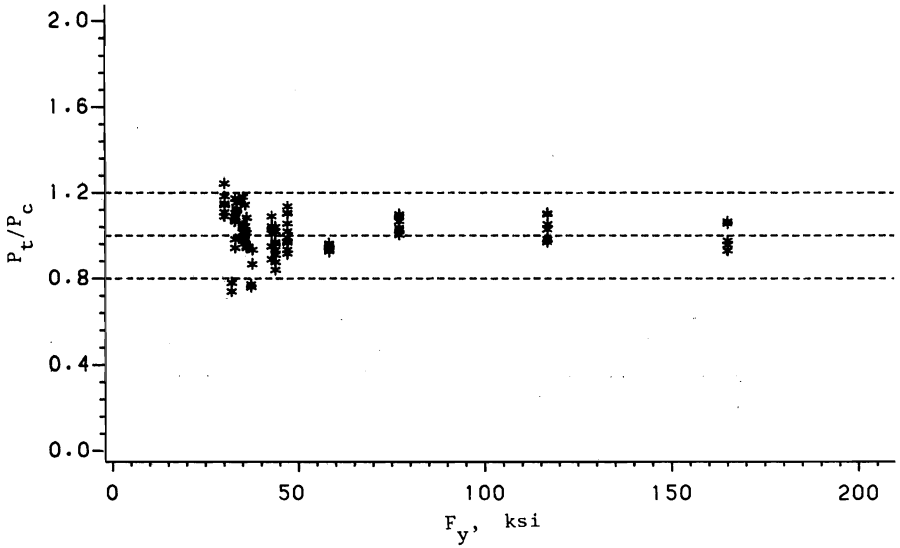

Fig. 6g Load Ratio, P_t/P_c, vs. Yield Strength, F_y, for I-Beams Subjected to Interior Two-Flange Loading

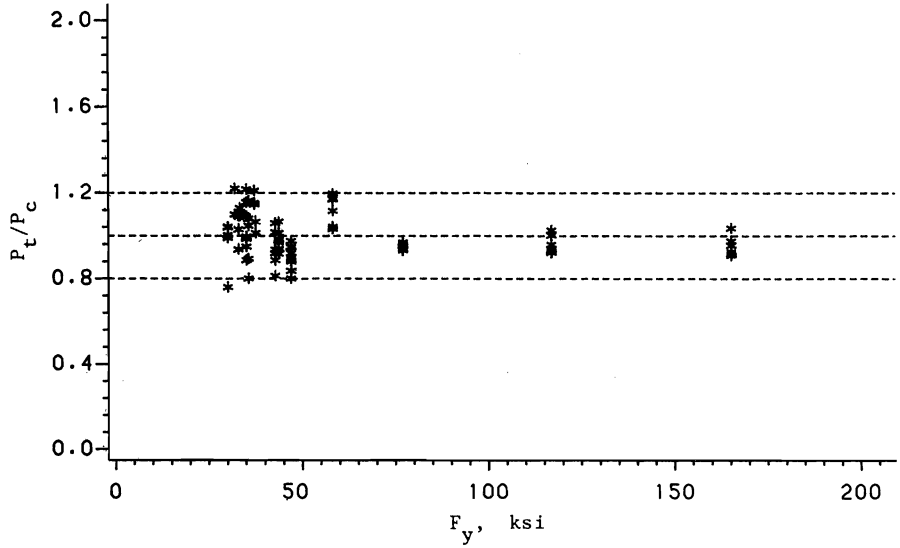

Fig. 6h Load Ratio, P_t/P_c, vs. Yield Strength, F_y, for I-Beams Subjected to End Two-Flange Loading

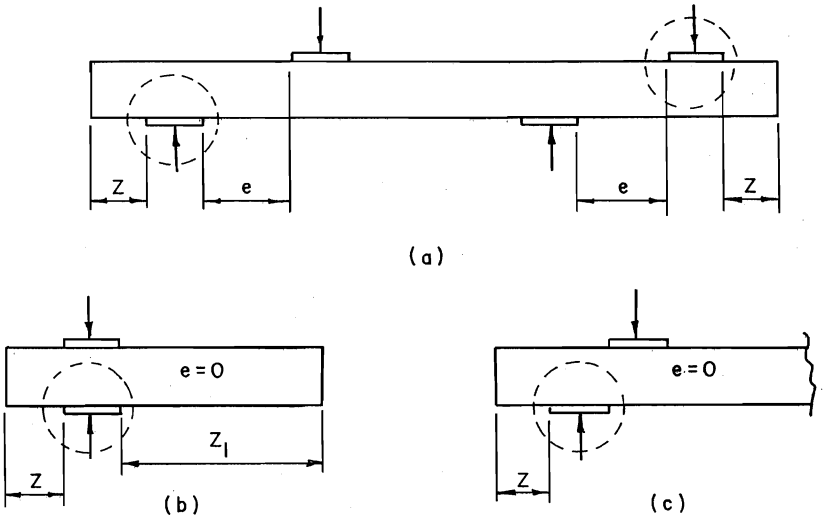

Fig. 7 Definitions of e and Z for Reactions and Concentrated Loads on Cantilevers

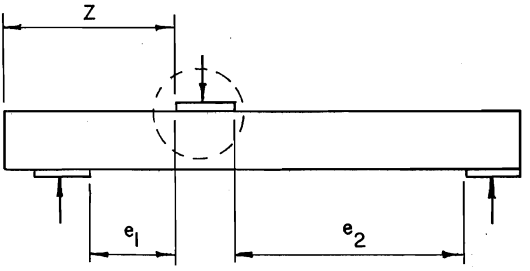

Fig. 8 Definitions of e and Z for Interior Concentrated Loads

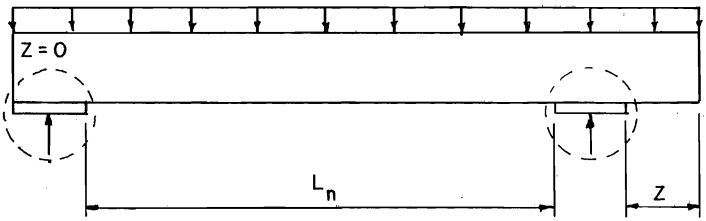

$e = L_n/2$

Fig. 9 Definitions of e and Z for End Reactions of Beams Supporting Uniformly Distributed Loads

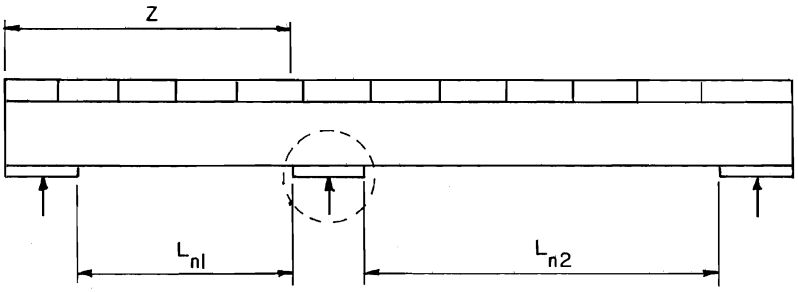

e = larger value of $L_{n1}/2$ and $L_{n2}/2$

Fig. 10 Definitions of e and Z for Interior Reactions of Continuous Beams Supporting Uniformly Distributed Loads